NDRG3 regulates imatinib resistance by promoting β-catenin accumulation in the nucleus in chronic myelogenous leukemia

XIAO WANG[1*], SIMIN RONG[1*], YUNXIAO SUN[2*], BAOHUI YIN[2], XIANCONG YANG[1], XIAOQING LU[2], HONGFANG SUN[1], YUNFEI YAN[1], GUANGBIN SUN[1], YAN LIANG[1], PINGYU WANG[1], SHUYANG XIE[1] and YOUJIE LI[1]

[1]Department of Biochemistry and Molecular Biology, Binzhou Medical University, Yantai, Shandong 264003; [2]Department of Pediatrics, Yantai Affiliated Hospital of Binzhou Medical University, Yantai, Shandong 264100, P.R. China

Received November 3, 2022; Accepted March 2, 2023

DOI: 10.3892/or.2023.8589

Abstract. Imatinib resistance in chronic myelogenous leukemia (CML) is a clinical problem. The present study examined the role of N-Myc downstream regulatory gene 3 (NDRG3) in imatinib resistance in CML. Quantitative PCR demonstrated that NDRG3 was highly expressed in patients with CML. Cell Counting Kit (CCK)-8 experiments proved that NDRG3 promoted the proliferation of K562 CML cells and enhanced imatinib resistance. Dual-luciferase assay showed that microRNA (miR)-204-5p inhibited expression of NDRG3 and immunofluorescence experiments showed that NDRG3 promoted accumulation of β-catenin in the nucleus, thereby increasing the expression of downstream drug resistance- and cell cycle-associated factors (c-Myc and MDR1). At the same time, cell proliferation experiments showed that β-catenin played a role in cell proliferation and drug resistance. Co-transfection with small interfering (si)-β-catenin partially reversed the effect of NDRG3. This finding indicated that NDRG3 plays an important role in imatinib resistance and miR-204-5p and β-catenin are involved in the biological behavior of NDRG3. The present results provide theoretical support for overcoming drug resistance in CML.

Introduction

Most cases of leukemia are acute lymphoid, acute myeloid leukemia or chronic myelogenous leukemia (CML) (1). CML has been used as a model cancer demonstrating the clinical benefit of targeted therapy and the ability of molecular diagnosis and monitoring (2). Dr Janet Rowley determined that a shortened chromosome 22 is formed after the mutual translocation between chromosome 9 and 22; ABL1 gene on chromosome 9 is inserted into the BCR region of chromosome 22; this translocation produces a fusion oncoprotein, BCR-ABL1 (3). The BCR-ABL chimeric gene is responsible for the production of BCR-ABL tyrosine kinase (4). Imatinib (IM) is a small molecule drug that competitively binds to the ATP-binding site of BCR-ABL. This inhibits the autophosphorylation of BCR-ABL, prevents its activation and blocks its downstream signaling (5). However, IM drug resistance and intolerance remain an issue in certain individuals, contributing to recurrence after treatment discontinuation (6). The N-Myc downstream-regulated gene (NDRG) family, which has four members, is functionally involved in multiple biological behaviors and can be used as a biomarker for various types of diseases, including prostate cancer, nervous system diseases and liver damage (7-9). NDRG2 plays an important role in cell proliferation, metastasis and apoptosis (10). NDRG3 is upregulated in tumor tissues (11-13). NDRG3 and the flexible loop corresponding to helix α6 of NDRG2 responsible for tumor suppression have structural differences leading to distinct roles, and this flexible loop region appears to play a unique role in NDRG3-induced oncogenic progression (14). As a key genetic element of lactate-dependent regulation, NDRG3 binds to lactate to maintain tumor progression and promote angiogenesis via the Raf/Erk pathway (15,16). At the same time, NDRG3 inhibits hypoxia-induced apoptosis (12). The role of a class of endogenous RNA molecules, microRNAs (miRNAs or miRs), has received extensive attention in cell biology (17,18). miRNAs are small non-coding RNAs that inhibit gene expression by binding to the 3' untranslated region (UTR) of target mRNAs and are involved in biological behaviors such as cell proliferation and migration; it has been reported that miRNAs are involved in drug resistance (19-21). NDRG3 is associated with drug resistance. The small nucleolar RNA host gene 20/miR-140-5p/NDRG3 axis is implicated in resistance to 5-fluorouracil in gastric cancer cell lines; miR-31 inhibits hepatocellular carcinoma (HCC) proliferation *in vitro* and *in vivo* and sensitizes HCC cancer cells to adri-70 doxorubicin

Correspondence to: Professor Youjie Li or Professor Shuyang Xie, Department of Biochemistry and Molecular Biology, Binzhou Medical University, 346 Guanhai Road, Yantai, Shandong 264003, P.R. China
E-mail: liyoujie@bzmc.edu.cn
E-mail: xieshuyang@bzmc.edu.cn

*Contributed equally

Key words: N-Myc downstream regulatory gene 3, β-catenin, chronic myelogenous leukemia, imatinib, microRNA-204-5p

by regulating its target gene NDRG3 (22,23). To the best of our knowledge, however, the role of NDRG3 in CML imatinib resistance has not been studied.

The upregulation of the Wnt signaling pathway has been implicated in tumorigenesis due to aberrant activation of β-catenin signaling, which is involved in cell metastasis, differentiation and drug resistance (24-26). In the cytoplasm, free β-catenin is typically transient, recognized by destruction complexes and rapidly targeted for degradation (27). The destruction complex contains the proteins glycogen synthase kinase 3β, adenomatous polyposis coli, casein kinase 1 and axin (28). When the degradation complex of β-catenin is converted into the active form, phosphorylated β-catenin is ubiquitinated and transported to the proteasome for degradation; when the degradation complex is inactive, β-catenin accumulates, flows into the nucleus to form a transcriptional complex with T cell-specific transcription factor/lymphoid enhancer-binding factor and initiates the transcription of downstream genes (29,30). β-catenin activates the transcription of c-Myc and cyclinD1, which are involved in cell proliferation and gene expression (27,31). Therefore, the present study investigated the role of β-catenin in IM resistance in CML to identify potential targets and mechanisms against drug resistance.

Materials and methods

Clinical samples. Patient and normal control samples were obtained from the Affiliated Hospital of Binzhou Medical University (Shandong, China). Sample collection was performed from October 2021 to January 2022. All patients were diagnosed with CML by pathology. The healthy controls had no physical disease or tumor. Subject information is shown in Table SI. The research protocol was approved by the Medical Ethics Committee of Binzhou Medical University (approval no. 2020-10-06) and the written informed consent of all subjects was obtained before study.

Cell culture. The human CML cell line K562 (Shanghai Yaji Biotechnology Co., Ltd.) was cultured in RPMI-1640 medium supplemented with 10% fetal bovine serum (both Gibco; Thermo Fisher Scientific, Inc.) and 1% penicillin-streptomycin (Beyotime Institute of Biotechnology) in a humid atmosphere containing 5% CO_2, 37˚C. K562 is a cell line isolated from the bone marrow of a 53-year-old patient with CML. We use K562 cells as the maternal cell line. K562 cells were treated with imatinib (IM) (Aladdin Industrial Corporation) to create the resistant K/G cells. K/G cells were incubated at 37˚C in 5% CO_2 in the presence of 10 μM IM for at least three days before the start of the experiment.

Lentiviral transduction. The lentiviral expression vector (pCDHNC or pCDHNDRG3; KeyyBio Sciences) and second-generation lentiviral packaging vectors (Addgene, Inc.) were transfected into 293T (Shanghai Cell Bank, Chinese Academy of Sciences, China) cells at 37˚C. The working solution (target plasmid: helper 1.0 plasmid: helper2.0 plasmid=16:12:8 μg) was placed into a 1.5 ml Eppendorf (EP) tube and 0.5 ml normal saline was added. At the same time, 10 μl VigoFect (Viglass Biotech) was added to another EP tube and supplemented with 0.5 ml normal saline. The two solutions were gently mixed and incubated for 15 min at 37˚C, placed into a petri dish and incubated at 37˚C and 5% CO_2. Duration of transfection was 6 h. Six hours after transfection, the cells were cultured in 1640 medium containing 10% serum. The virus supernatant was collected after 24 h, 48h and 72 h. Cell debris was removed by centrifugation at 4,000 g for 10 min at 4˚C. K/G cells were infected at an MOI of 20 with polybrene (Sigma Aldrich; Merck KGaA) and lentiviral particles. Transfection was performed at a cell density of 70-80% in six-well plates in a 37˚C, 5% CO_2 incubator. Infection efficiency was assessed by observing the expression of GFP using a fluorescence microscope. After infected with lentivirus for 6-8 h, the cells were replaced with 1640 medium with 10% serum for culture. Follow-up experiments were carried out after 24-48 h. Transduction into target cells can last 48-72 h. The empty plasmid served as a negative control (NC). The plasmid vectors were from GenePharma Company. The sequences were as follows: NC forward, 5'-GTTCTCCGAACGTGTCACGT(T)-3' and reverse, 5'-AACGTGACACGTTCGGAGAACTT-3'; small interfering (si)-NDRG3 forward, 5'-AGGAAGAGTTAC AGGCCAATT-3' and reverse, 5'-TTGGCCTGTAACTCT TCCT(T)-3'; si-β-catenin forward, 5'-TGGTTAATAAGG CTGCAGTTATTTCAAGAGAATAACTGCAGCCTTATT AACCTTTTTTC-3' and reverse, 5'-TCGAGAAAAAAG GTTAATAAGGCTGCAGTTATTCTCTTGAAATAACTG CAGCCTTATTAACCA-3'; miR-204-5p-mimic forward, 5'-TTCCCTTTGTCATCCTATGCCT-3' and reverse, 5'-AGG CATAGGATGACAAAGGGAA(TT)-3' and miR-204-5p-inhibitor, 5'-AGGCATAGGATGACAAAGGGAA(TT)-3'.

Cell Counting Kit (CCK)-8 assay. Following transfection, a bovine abalone counter was used to count K562 and K/G cells. Cells were plated into 96-well flat bottom plates at $2x10^3$ cells/well with or without 16 μM IM treatment at 37˚C, 24 h. After cells were cultured for 0, 24, 48 and 72 h at 37˚C, the cell proliferation was determined using the CCK-8 kit (Beyotime Institute of Biotechnology).

K/G cells were plated into 96-well flat bottom plates at $2x10^3$ cells/well with or without IM (0, 1, 2, 4, 8, 16, 32, 64 and 128 μM) for 24 h at 37 ˚C. CCK-8 reagent was added to the cultured cells for 2 h. The absorbance at 450 nm was determined using a microplate reader (Multiskan FC; Thermo Fisher Scientific, Inc.). The cell viability curve was constructed and the half-maximal inhibitory concentration (IC_{50}) was obtained using GraphPad Prism 8 software (GraphPad Software, Inc.).

Western blot analysis. Cell and tissue proteins were extracted using RIPA (Beyotime Biotechnology). Protein concentration was detected by the BCA kit and the protein loading was 10-40 μg. Proteins were separated by using a 10% gel for polyacrylamide gel electrophoresis, and transferred to polyvinylidene fluoride membranes and blocked for 2 h with 5% skimmed milk at room temperature. Then, proteins on the membrane were detected with primary antibodies for 16-18 h at 4˚C, including anti-β-catenin (1:1,000; cat. no. bsm-33194M; BIOSS), anti-NDRG3 (1:750; cat. no. BS62436; Bioworld Technology, Inc.), anti-c-Myc (1:6,000; ca. to. 10828-1-AP; Proteintech Group, Inc.), anti-MDR1 (1:1,000; ca. to. 13342S;

Cell Signaling Technology), anti-LaminB1 (1:6,000; cat. no.12987-I-AP; Proteintech Group, Inc.) and anti-GAPDH (1:6,000; cat. no. BS65483M; Bioworld Technology, Inc.). After 2 h of incubation with goat anti-rabbit IgG H&L HRP conjugate secondary antibody (1:6,000; cat. no. BS13278; Bioworld Technology, Inc.) at 4˚C, protein bands were visualized using BeyoECL Plus (Beyotime Institute of Biotechnology). Finally, the densitometric analysis of the protein was performed using ImageJ software (National Institutes of Health, Bethesda, MD, USA).

Reverse transcriptionquantitative (RTq)PCR. RNA was extracted from cells and tissues on ice using TRIzol® reagent (Thermo Fisher Scientific, Inc).According to the manufacturer's protocol, reverse transcription of RNA was performed to generate cDNA using PrimeScript RT Kit (Takara Bio, Inc). Reagents for RT-qPCR (SYBR® Mix ExTaq™ II) were obtained from Takara Bio, Inc. Thermocycling conditions were as follows: Initial denaturation at 95˚C for 2 min, followed by 40 cycles of denaturation at 95˚C for 15 sec, annealing at 60˚C for 30 sec and extension at 72˚C for 30 sec.

5S rRNA was used as the internal reference gene of miRNA. GAPDH was used as the internal reference gene of mRNA and the $2^{-\Delta\Delta Cq}$ method was used for normalization (32). Primers used for RT-qPCR are shown in Tables SII and SIII. The analysis of clinical samples was performed based on the change in cycle threshold (ΔCq) between the target gene NDRG3 and housekeeping gene GAPDH using $2^{-\Delta Cq}$ (33).

Flow cytometric analysis. Treated K/G cells were seeded into 6-well plates at a density of 70-80% and cultured for 48 h at 37˚C. Then, cells were fixed with 70% ethanol for 12-16 h at 4˚C and stained with propidium iodide (PI/RNaseA, Nanjing KeyGen Biotech Co., Ltd.) for 30-60 min at room temperature. Cell cycle distribution was analyzed using a BD Accuri™ C6 Plus Flow Cytometer (BD Biosciences) and ModFitLT4.0 mapping (Verity Software House).

Luciferase activity assay. Based on the wild-type (wt) binding site between miR-204-5p and NDRG3 (determined via Targetscan7.1; targetscan.org/vert_71/), the mutant (mut) sequence fragment of NDRG3 was designed. Luciferase reporter plasmids, including NDRG3-3'-UTR-wt and NDRG3-3'-UTR-mut, were constructed by GenePharma The sequences were as follows: NC,5'-GTTCTCCGAACGTGTCACGT(T)-3'; miR-204-5p, 5'-TTCCCTTTGTCATCCTATGCCT-3'. The plasmid vectors were from GenePharma Company. For dual-luciferase reporter assays, 293T cells were transfected with miR-204-5p or NC and NDRG3-3'-UTR-wt or NDRG3-3'-UTR-mut and incubated by using Lipofectamine 2000® reagent (Invitrogen; Thermo Fisher Scientific, Inc) for 4-8 h. Duration between transfection and activity measurement was 48 h. Then, cells were harvested and lysed on ice. The luciferase activity was measured using a Dual-Glo® Luciferase Assay System (Promega Corporation). Firefly luciferase activity was normalized to Renilla luciferase activity.

Immunofluorescence. Sterilized cover slips were placed onto 24-well plates. Gelatin-coated solution (400 μl, Sigma Aldrich, USA) was added for 10 min at room temperature. Excess gelatin-coated solution was aspirated and coverslips were air-dried for 15 min. Dry cover slips were stored at room temperature until use. Treated 293T cells were seeded onto gelatin coverslips at a cell density of 50-60%, which were prewashed three times with Phosphate Buffered Saline (PBS). The formaldehyde fixative (300-400 μl, 2-4%) was added to each well and incubated for 20 min at room temperature. Coverslips containing fixed cells were washed twice with 400 μl PBS). Non-specific staining was blocked by the addition of 400 μl fluids (1% BSA+0.2% TritonX-100, PBS) and incubated for 1 h at room temperature. coverslips were then incubated with mouse anti-β-catenin (1:100; cat. no. bsm-33194M; BIOSS) and anti-NDRG3 (1:100; cat. no. BS62436; Bioworld Technology, Inc.) at 37˚C for 2 h. Alexa fluor conjugate secondary antibodies (1:100, Donkey-anti-Rabbit IgG-Alexa fluor 594, cat. no. abs20021, absin and 1:100, goat anti-mouse IgG H&L/Alexa Fluor 488, cat. no. bs-0296G-AF488, BIOSS) were incubated at 37˚C for 2 h and stained with DAPI (10 μg/ml, Solarbio) for 5-10 min at room temperature. Images were captured by confocal microscopy at 400X magnification. The same microscope/software intensity parameters were used for both groups.

Extraction of cytoplasmic and nuclear protein. K/G cells were washed once with PBS and centrifuged by using Legend Micro 17R centrifuge (Thermo Scientific) at 500 x g, 4˚C for 2-3 min. The supernatant was aspirated and the pellet was retained. A total of 200 μl cytosol protein extraction kit (Beijing Solarbio Science & Technology Co., Ltd)/20 μl cell pellet (~$2x10^6$ cells) was added, placed on ice for 10 min after pipetting evenly and centrifuged at 12,000 g and 4˚C for 10 min. The supernatant contained plasma protein. The remaining precipitate was added to 50-100 μl nuclear protein extraction kit (Beijing Solarbio Science & Technology Co., Ltd). the procedure used to extract plasma proteins was used to extract nucleoprotein; the obtained supernatant contained nucleoprotein, which was used for subsequent experiments.

Immunoprecipitation. According to the requirements of the reagent manufacturer, the nuclear protein extraction kit (Beijing Solarbio Science & Technology Co., Ltd) was used to extract the nucleoprotein, and the cells in a 10 cm culture dish need 800-1,000 μl the lysate. and centrifuged at 12,000 g for 10 min at 4˚C. Nuclear extracts were incubated on a rotator with 8-10 μl anti-β-catenin overnight at 4˚C. The anti-β-catenin antibody was used for protein blotting (1:100; cat. no. A19657; ABclonal Biotech Co, Ltd). A total of ~10 μl protein A/G agarose beads (cat. no. PR40025; Proteintech Group, Inc.) was added and the IgG control was detected by western blotting. The washing buffer was Tris-Buffered Saline and 0.1% Tween20 (TBST). The protein-antibody protein A/G-agarose bead complexes were boiled to achieve separation. Western blot verification was then carried out.

Animal model. A total of 40 female nude mice (weighing 18 g were purchased from Jinan Pengyue Company (BALB/c-nu; age, 5 weeks) and they were kept in a laminar airflow cabinet under specific pathogen-free conditions with a controlled temperature (23±2˚C), 12/12-h light/dark cycle and humidity (40-70%) with free access to food and water. Nude mice were divided into experimental groups (n=5/group) with different treatments (pLV-NC, pLV-miR-204-5p-mimic; pLV-NC,

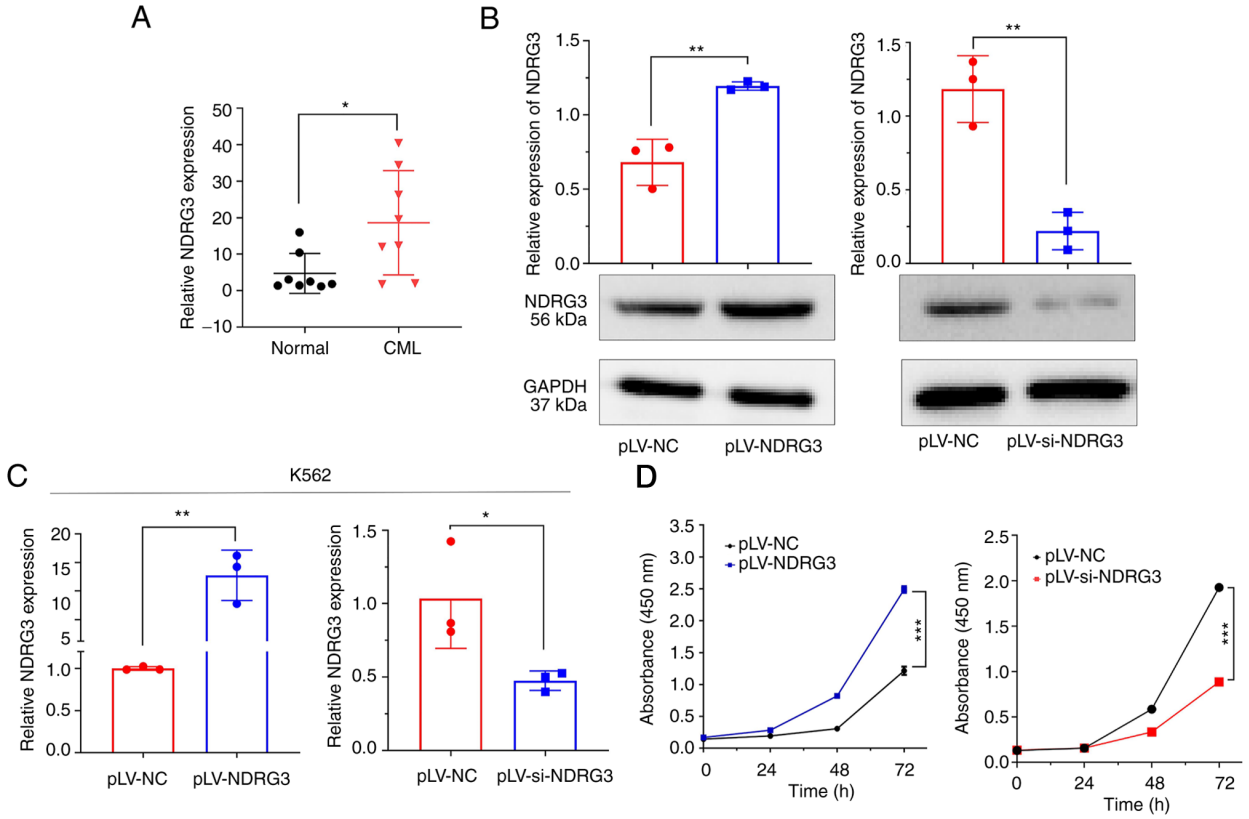

Figure 1. Expression of NDRG3 is associated with cell proliferation in CML. (A) Differential expression of NDRG3 in patients with CML and normal controls (both n=8). (B) Protein expression of NDRG3 was assessed by western blot. (C) mRNA expression of NDRG3 following the overexpression and knockdown of lentiviral plasmid vectors was assessed by reverse transcriptionquantitative PCR. The histogram shows the comparison of the relative intensity of NDRG3 and GAPDH. (D) Cell Counting Kit8 assay of proliferation of K562 cells following lentivirus infection with NDRG3. *P<0.05, **P<0.01 and ***P<0.001. NDRG3, N-Myc downstream-regulated gene 3; NC, negative control; CML, chronic myelogenous leukemia; si, small interfering.

pLV-miR-204-5p-inhibitor; pLV-NC, pLV-si-NDRG3; pLV-NC + IM, pLV-si-NDRG3 + IM). A total of ~5x10^{6} K/G cells was resuspended into 50 μl PBS mixed with 50 μl Matrigel (BD Biosciences) and subcutaneously into the back of nude mice. For IM treatment, 10 mice were intraperitoneally injected with IM (50 mg/kg) after the tumor grew to the seventh day. Injection once on the fourteenth day, and once on the twenty-first day, a total of three times. The health and weight of mice were monitored every day. Tumor volume was measured every 5 days. After 25 days, 40 mice were euthanized by injection of sodium pentobarbital (150-200 mg/kg). The tumor tissue was excised, photographed and stored for western blotting. Animal experiments were reviewed and approved by the Animal Ethics Committee of Binzhou Medical University (Yantai, China; approval no. 2020-10-06).

Intervention. Inhibitor of β-catenin-responsive transcription 14 is abbreviated as iCRT14 (MedChemExpress). K/G cells were transfected, and the groups were NDRG3+DMSO (Solarbio) and NDRG3+iCRT14. The concentration of iCRT14 was 1 mM (dissolved in DMSO), added iCRT14 after transfection 24 hours, and the final concentration was 25 μM. The experiment was performed after another 24 h.

miRNAs databases. Targetscan database (targetscan.org/vert_71/), miRdb (mirdb.org/index.html), mirDIP (ophid.utoronto.ca/mirDIP/) and miRWalk (mirwalk.umm.uni-heidelberg.de/) were used to screen miRNAs targeting NDRG3.

Statistical analysis. Data are presented as the mean ± standard deviation. One-way ANOVA and Student's t test were used to compare differences between three and two groups, respectively. Tukey's post hoc test was used following ANOVA. Unpaired t-tests were used. All statistical tests were two-sided. P<0.05 was considered to indicate a statistically significant difference. GraphPad Prism 8 software was used for all data analysis.

Results

Expression of NDRG3 is associated with cell proliferation in CML. Expression of NDRG3 was assessed in patients with CML and normal controls (both n=8) by RT-qPCR; NDRG3 was more highly expressed in patients with CML (Fig. 1A). Next, the effects of overexpression and knockdown of NDRG3 on mRNA and protein levels in K562 cells were assessed by RT-qPCR and western blotting. NDRG3 was successfully overexpressed and knocked down (Fig. 1B and C). IC_{50} in K562 cells was 0.2125 μM (Fig. S1). CCK-8 assay confirmed that compared with the control, the downregulation of NDRG3 significantly inhibited the proliferation of K562 cells, whereas NDRG3 overexpression promoted the proliferation of K562 cells (Fig. 1D).

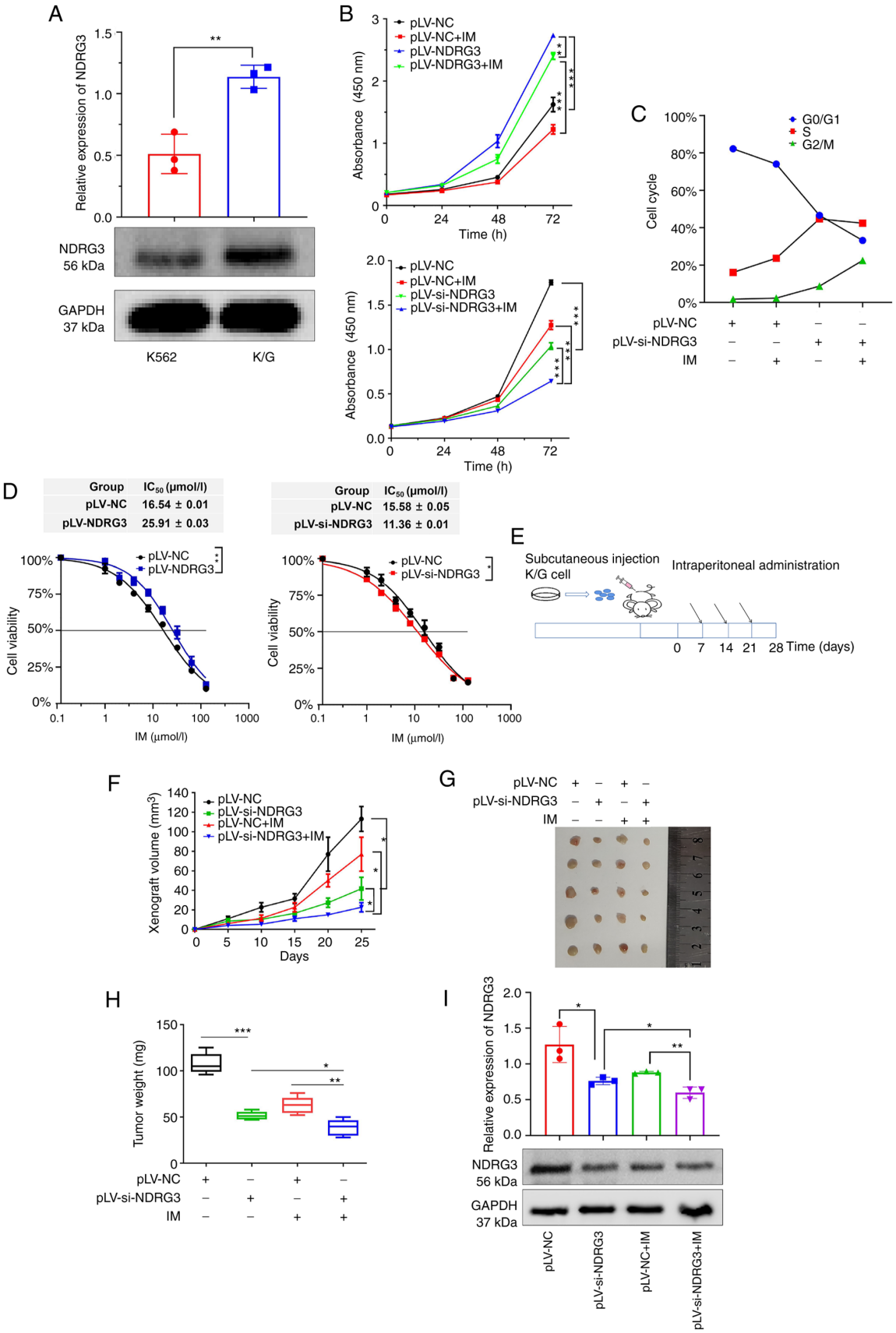

Figure 2. NDRG3 promotes cell proliferation and drug resistance *in vitro* and *in vivo*. (A) NDRG3 expression in K562 and K/G cells. (B) Cell proliferation after NDRG3 and IM treatments at 0, 24, 48, and 72 h, as shown by the CCK-8 assay. (C) Determination of cell cycle progression following NDRG3 and IM treatment by flow cytometry. (D) Detection of IC50 by CCK-8 assay after transfection of NDRG3. (E) Experimental timeline of tumor-bearing nude mice. (F) Monitoring of tumor growth by using tumor volume. (G) Representative images of tumor tissue. (H) Monitoring of tumor growth by using tumor weight. (I) Expression of NDRG3 protein in tumor tissues of nude mice shown by western blotting. The histogram shows relative intensity of NDRG3 and GAPDH. *P<0.05, **P<0.01, and ***P<0.001. NDRG3, N-Myc downstream-regulated gene 3; CCK8, Cell Counting Kit8; IM, imatinib; IC_{50}, half-maximal inhibitory concentration; NC, negative control; si, small interfering.

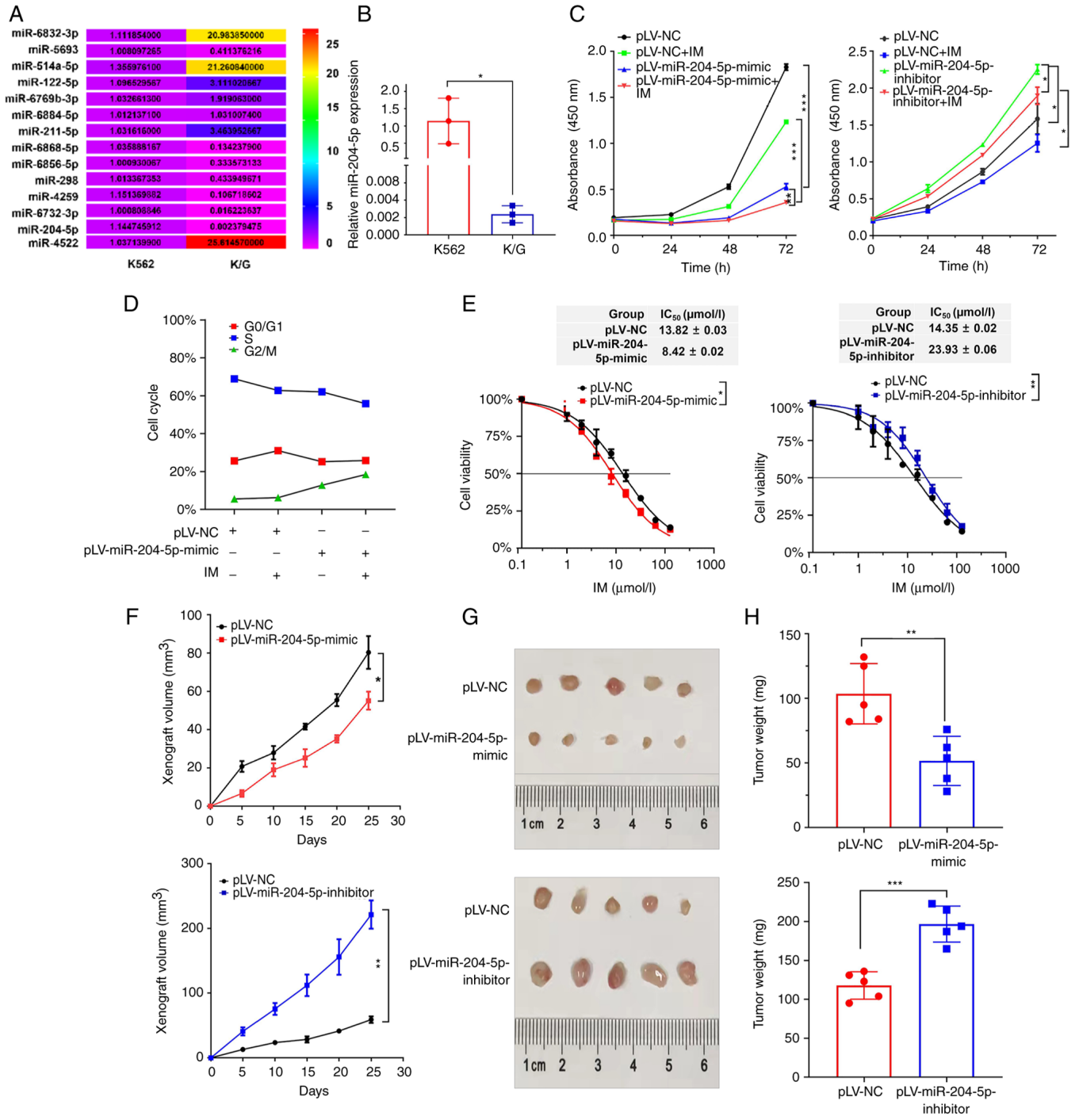

Figure 3. miR-204-5p suppresses cell proliferation and drug resistance. (A) Screening of miRs targeting NDRG3. (B) Expression of miR-204-5p in K562 and K/G cells. (C) Detection of cell viability changes following treatment with miR-204-5p + IM by Cell Counting Kit-8 assay. (D) Cell cycle distribution after overexpression of miR-204-5p in K/G cells. (E) IC_{50} following lentiviral overexpression and knockdown of miR-204-5p in K/G cells. (F) Subcutaneous injection of K/G cells into nude mice to construct tumor models. (G) Volume of xenograft tumors. (H) The tumor of nude mice were weighed. *P<0.05, **P<0.01 and ***P<0.001. NDRG3, N-Myc downstream-regulated gene 3; IM, imatinib; IC_{50}, half maximal inhibitory concentration; miR, microRNA; NC, negative control.

NDRG3 promotes cell proliferation and drug resistance in vitro and in vivo. Western blotting showed expression of NDRG3 in K/G cells was higher than that in K562 cells, which suggested that NDRG3 may be involved in drug resistance (Fig. 2A). NDRG3 knockdown group showed significantly inhibited proliferation of K/G cells and NDRG3 knockdown + IM exhibited a notable inhibitory effect. The NDRG3 overexpression group promoted proliferation, but this was attenuated when NDRG3 co-acts with IM (Figs. 2B and S2A and B). The cell cycle analysis revealed that the NDRG3 knockdown group had a higher proportion of G2/M phase cells compared with the control group (Fig. 2C). Growth curves showed that the IC_{50} of IM was elevated in NDRG3-overexpressing cells compared with untreated cells (Fig. 2D). The role of NDRG3 was verified by nude mouse xenograft experiments (Fig. 2E). The tumor growth curve showed the slowest growth in NDRG3 knockdown + IM group (Fig. 2F). Knockdown of NDRG3 + IM group had the smallest tumor weight (Fig. 2G and H). Finally,

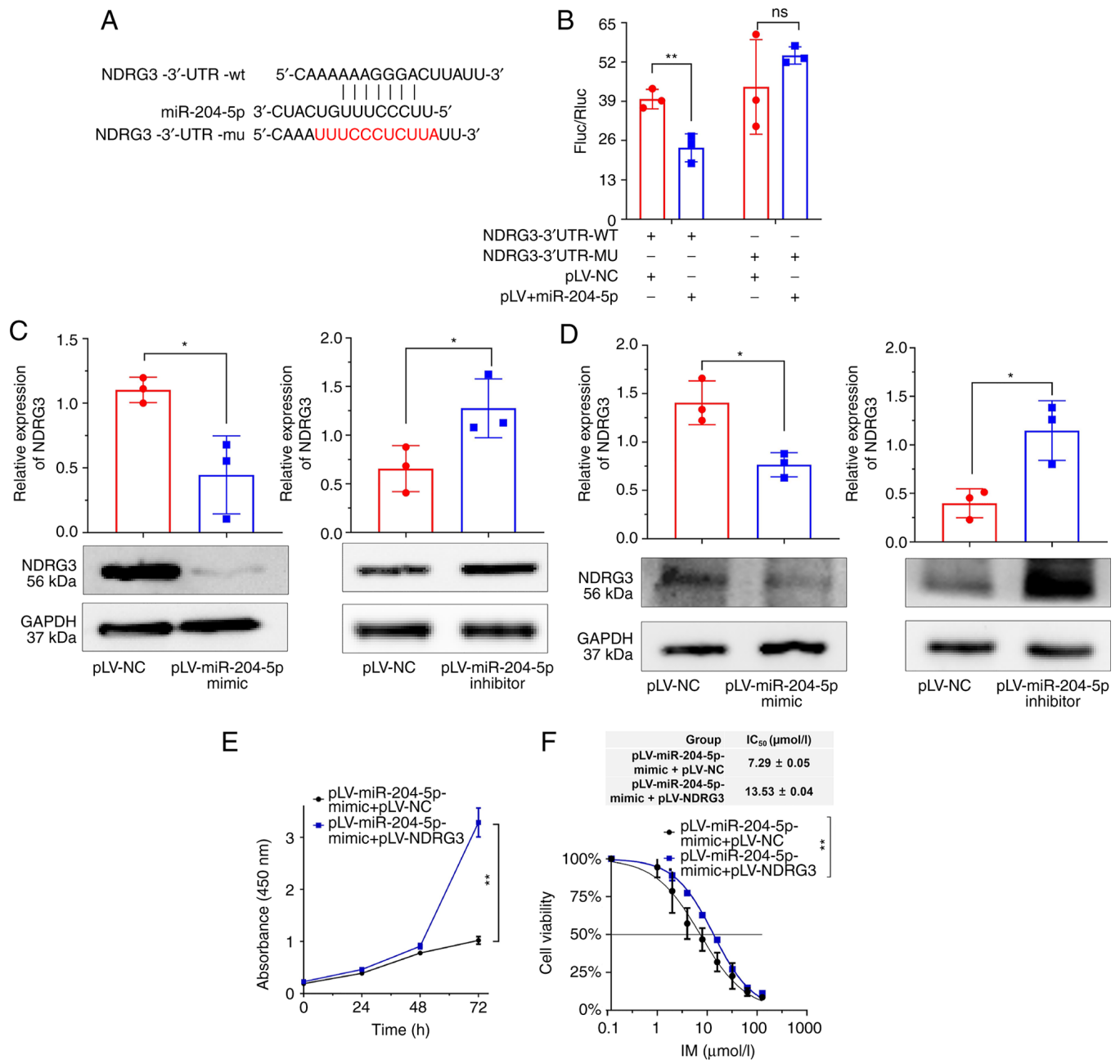

Figure 4. miR-204-5p targets NDRG3. (A) Sequence fragments of NDRG3-3'-UTR-wt and NDRG3'-UTR-mut. Positions 404-410 of the NDRG3-3'-UTR have a binding site for miR-204-5p. Mutation at positions 404-414 of the NDRG3-3'-UTR. (B) Association between miR-204-5p and NDRG3 validated by dual-luciferase reporter gene analysis. (C) Western blot analysis of expression changes in NDRG3 after miR-204-5p treatment in K/G cells. The histogram shows relative intensity of NDRG3 and GAPDH. (D) NDRG3 of expression changes in tumor tissue. The histogram shows relative intensity of NDRG3 and GAPDH. (E) Cell viability and (F) IC_{50} after co-transfection of miR-204-5p and NDRG3 assessed by Cell Counting Kit-8 assay. $^{*}P<0.05$, $^{**}P<0.01$. NDRG3, N-Myc downstream-regulated gene 3; IC_{50}, half-maximal inhibitory concentration; miR, microRNA; UTR, untranslated region; wt, wild-type; mut, mutant; ns, not significant; Fluc, firefly luciferase; Rluc, *Renilla* luciferase; NC, negative control.

the pLV-si-NDRG3 + IM group had the lowest NDRG3 protein expression in tumor tissue (Fig. 2I). These results indicated that NDRG3 promoted cellular IM resistance and proliferation *in vitro* and *in vivo*.

miR-204-5p suppresses cell proliferation and drug resistance. To screen for miRNAs that may target NDRG3 and participate in IM response, multiple databases were searched, which identified 14 miRNAs (Fig. 3A). miRNAs in K562 and K/G cell lines were analyzed by RT-qPCR; miR-204-5p expression was lowest in K/G cells compared with K562 cells (Figs. S3A and B). The proliferation of K/G cells in the IM, pLV-miR-204-5p-mimc and pLV-miR-204-5p-mimic + IM groups was markedly decreased compared with that in the pLV-nc group. Furthermore, pLV-miR-204-5p-mimic + IM-tre ated cells exhibited a lower decrease in proliferation compared with IM-treated cells. The miR-204-5p-inhibitor group demonstrated that the cell proliferation was enhanced (Figs. 3C and S3B). The cell cycle assay indicated that entry into G2/M phase was inhibited after overexpression of miR-204-5p; this

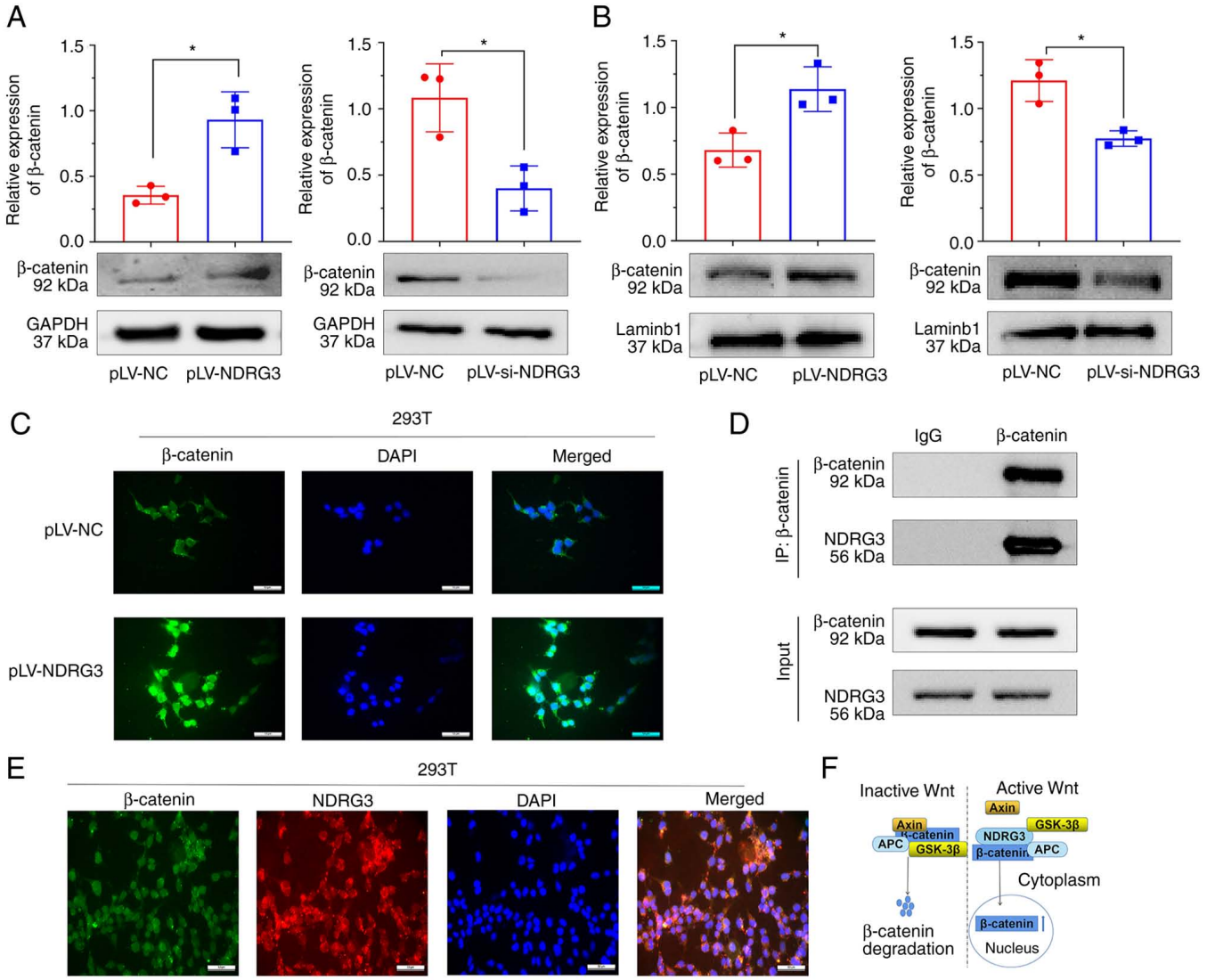

Figure 5. NDRG3 promotes accumulation of β-catenin in the nucleus. (A) Western blot analysis using whole cell lysate of β-catenin protein expression levels in K/G NDRG3-overexpressing and -knockdown cells. Histogram shows the comparison of the relative intensity of β-catenin and GAPDH. (B) Relative nuclear β-catenin expression in pLV-NDRG3 or pLV-si-NDRG3 K/G cells demonstrated by western blotting using nuclear extract. The histogram shows the comparison of the relative intensity of β-catenin and LaminB1. (C) β-catenin protein levels following NDRG3 overexpression obtained by immunofluorescence analysis. Scale bar, 50 μm. (D) IP of K/G cell nuclear extract. Normal IgG was used as a control. (E) 293T cells stained with anti-NDRG3 (red) and anti-β-catenin antibody (green). Immunofluorescence was used to analyze co-localization of NDRG3 and β-catenin protein in 293T cells. Scale bar, 50 μm. (F) Schematic of the β-catenin degradation complex. *P<0.05. NDRG3, N-Myc downstream-regulated gene 3; si, small interfering; NC, negative control; IP, immunoprecipitation; GSK, glycogen synthase kinase; APC, adenomatous polyposis coli.

effect was stronger after combination with IM (Fig. 3D). It was investigated whether miR-204-5p-mimic increases IM sensitivity in CML cells. IC_{50} of the miR-204-5p-mimic group was 8.422 μM in K/G cells and IC_{50} of the miR-204-5p-inhibitor group was 23.93 μM (Fig. 3E).

The effect of miR-204-5p was verified *in vivo* by tumor-bearing experiments in nude mice; compared with that in the control group, tumor growth was slower in the miR-204-5p overexpression group and faster in the miR-204-5p knockdown group (Fig. 3F). Compared with the control group, tumor weights of the overexpression and knockdown groups were smaller and larger, respectively (Fig. 3G and H).

miR-204-5p targets NDRG3. To demonstrate that miR-204-5p targets NDRG3, wt and mut NDRG3 3'-UTR regions were constructed (Fig. 4A). Dual-luciferase reporter gene assay showed that miR-204-5p targeted the 3'-UTR of NDRG3 (Fig. 4B). miR-204-5p-mimic significantly decreased NDRG3 protein levels in cells and tumor tissue (Fig. 4C and D). Cell proliferation experiments showed that the inhibitory effect of miR-204-5p on cell proliferation and drug resistance was alleviated following co-transfection with miR-204-5p-mimic with NDRG3 (Fig. 4E and F). In summary, these results suggested that miR-204-5p inhibited the expression of NDRG3 and that NDRG3 overexpression abolished the effect of miR-204-5p.

NDRG3 promotes accumulation of β-catenin in the nucleus. The mechanism by which NDRG3 promoted drug resistance in CML was investigated. Western blotting using whole cell lysates showed that the expression of β-catenin was significantly increased and decreased by NDRG3 overexpression and downregulation, respectively (Fig. 5A). Western blot using

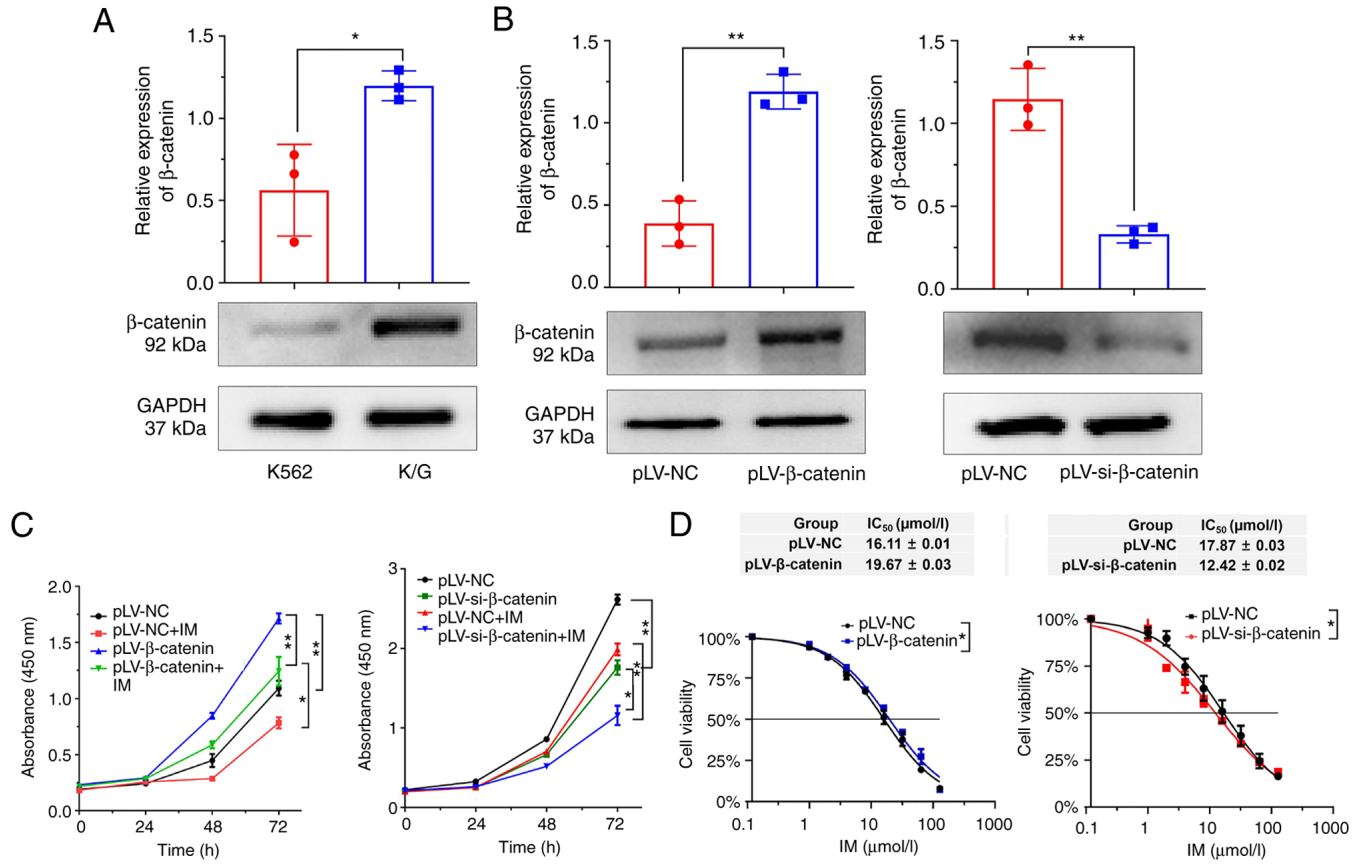

Figure 6. β-catenin promotes cell proliferation and drug resistance. (A) β-catenin expression in K562 and K/G cells assessed by western blot. The histogram shows the relative intensity of β-catenin and GAPDH. (B) Efficiency of overexpression and knockdown of β-catenin. The histogram shows relative intensity of β-catenin and GAPDH protein. (C) Detection of cell proliferation after treatment of β-catenin combined with IM by Cell Counting Kit-8 assay. (D) IC_{50} after lentivirus infection with β-catenin. *P<0.05, **P<0.01. IM, imatinib; IC_{50}, half-maximal inhibitory concentration; NC, negative control; si, small interfering.

nuclear extracts found that the overexpression of NDRG3 further increased expression of β-catenin in the nucleus (Fig. 5B). The nucleus accumulation of β-catenin in 293T cells increased after NDRG3 overexpression compared with controls (Fig. 5C). β-catenin was shown to be co-expressed with NDRG3 by immunoprecipitation of nuclear extracts (Fig. 5D). Immunofluorescence staining showed that NDRG3 and β-catenin were co-localized in the cytoplasm of 293T cells Fig. 5E). The schematic diagram of β-catenin functioning was shown in Fig. 5F. The mRNA levels of c-Myc and MDR1 was increased, and the protein expression of c-Myc and MDR1 was increased following overexpression of NDRG3 (Fig. S4A and B).

β-catenin enhances cell proliferation and drug resistance. Expression of β-catenin in K/G cells was higher than that in K562 cells (Fig. 6A). β-catenin was successfully knocked down (Fig. S5) and the knockdown of β-catenin enhanced the antitumor activity of IM, as shown by cell proliferation experiments (Figs. 6B and C). CCK-8 assay showed that β-catenin knockdown could decrease IM resistance in CML cells (Fig. 6D). These results indicated that β-catenin was involved in cell proliferation and drug resistance.

β-catenin reverses the effects of NDRG3 on cell proliferation and drug resistance. To verify whether NDRG3 functions via the β-catenin signaling pathway, iCRT14 was used. β-catenin was inhibited at the protein level after adding the inhibitor (Fig. 7A). CCK-8 experiment found that the inhibitor suppressed the ability of NDRG3 to promote cell proliferation and IM resistance (Fig. 7B and C). In summary, the effect of NDRG3 on β-catenin was weakened after adding the inhibitor. Western blot showed that the expression of β-catenin protein decreased after the co-transfection of pLV-NDRG3 and pLV-si-β-catenin (Fig. 7D). The inhibitory effect of β-catenin abolished the ability of NDRG3 to promote cell proliferation and IC_{50} was decreased following co-transfection of pLV-si-β-catenin and pLV-NDRG3 (Fig. 7E and F). β-catenin knockdown reversed the effect of NDRG3 on K/G cell resistance. The potential mechanism is shown in Fig. 8. β-catenin is degraded when the Wnt signaling pathway is inactive (34), but β-catenin will accumulate in the nucleus under the action of NDRG3. As a result, it leads to increased expression of downstream factors, including c-Myc and MDR1, and initiates downstream biological behaviors such as cell proliferation and drug resistance. miR-204-5p regulates the expression of NDRG3.

Discussion

Previous studies have suggested that NDRG3 serves a role in tumor growth in hepatocarcinogenesis and osteosarcoma (23,35). However, NDRG3 plays a tumor suppressor role in prostate cancer (7). Conflicting data may be attributed

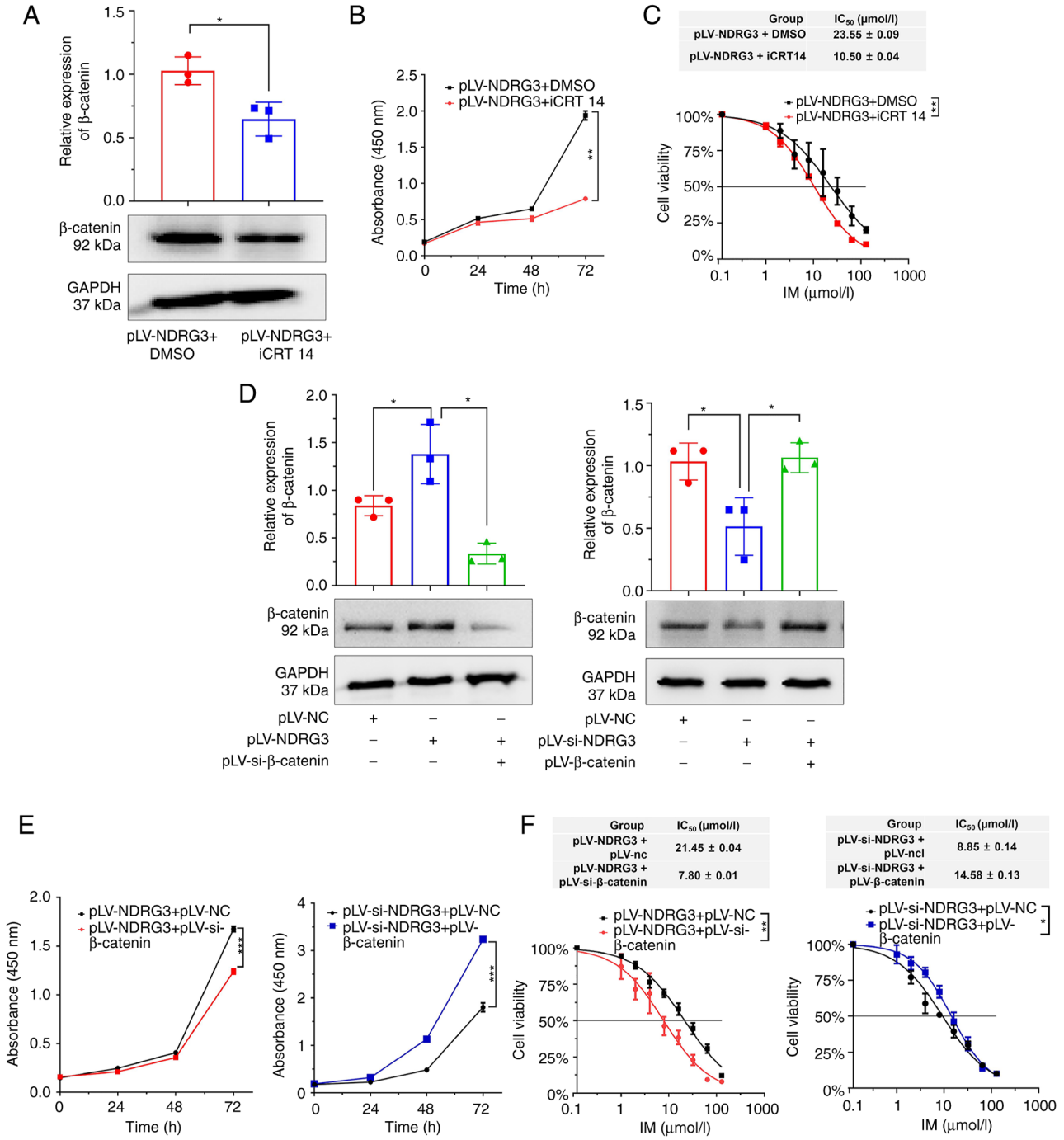

Figure 7. β-catenin reverses the effects of NDRG3 on cell proliferation and drug resistance. (A) Protein expression of β-catenin following transfection and iCRT14 treatment assessed by western blot. The histogram shows the comparison of the relative intensity of β-catenin and GAPDH. (B) Cell proliferation ability and (C) IC_{50} following transfection and iCRT14 treatment. (D) Protein expression of β-catenin following transfection detected by western blot. The histogram shows relative intensity of β-catenin and GAPDH. (E) Cell viability and (F) IC_{50} following co-transfection with si-β-catenin. $^{*}P<0.05$, $^{**}P<0.01$ and $^{***}P<0.001$. NDRG3, N-Myc downstream-regulated gene 3; iCRT14, inhibitor of β-catenin responsive transcription 14; IC_{50}, half-maximal inhibitory concentration; si, small interfering; NC, negative control.

to differences in the tumor microenvironment, tumor type or experimental approaches (36). A previous study demonstrated NDRG3 is a hypoxia-induced lactate sensor and the lactate/NDRG3/Raf/ERK signaling pathway may underlie hypoxia-associated physiological and pathophysiological responses (12). The present results showed that expression of NDRG3 in patients with CML was higher than that in normal controls and promoted K562 cell proliferation. The problem of drug resistance in cancer diagnosis and treatment is a key obstacle to successful treatment (37). 7-Ketocholesterol is an oxidized cholesterol derivative that improves vincristine and doxorubicin cytotoxicity through a classical MDR-regulated mechanism in CML (38). Vandetanib, an oral multiple tyrosine kinase Inhibitor (TKI), inhibits acute myeloid leukemia cells proliferation and overcomes IM resistance in CML by targeting ephrin type-B receptor 4 (EPHB4) (39). In the present study, compared with K562 cells, K/G cells exhibited greater IM resistance. NDRG3 was highly expressed in

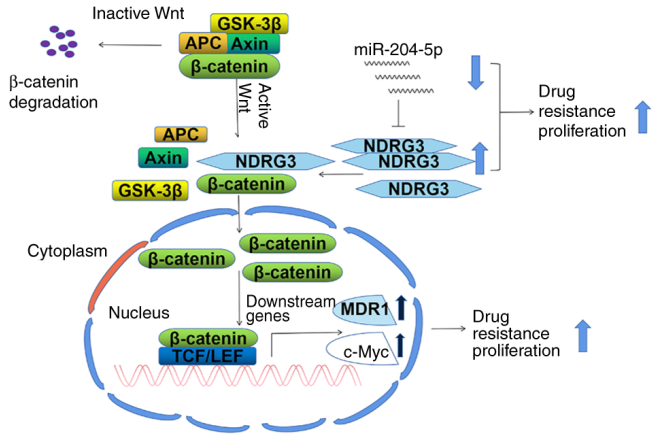

Figure 8. Molecular mechanism by which NDRG3 works. GSK, glycogen synthase kinase; APC, adenomatous polyposis coli; NDRG3, N-Myc downstream-regulated gene 3; miR, microRNA; MDR1, Multidrug resistance gene 1; TCF/LEF, T cell-specific transcription factor/lymphoid enhancer-binding factor.

IM-resistant cell lines. When NDRG3 was overexpressed, the IC_{50} of K/G cells significantly increased, which means that NDRG3 increased IM resistance. The present data suggested that NDRG3 exerted a clear role in promoting imatinib resistance. In other studies, it was found that there are multiple ways to regulate drug resistance, such as drug action, protein regulation, kinase stimulation and autophagy (40-43). The aforementioned results showed that NDRG3 plays a role in CML cell proliferation and drug resistance.

Gene expression is regulated by miRNAs. For example, miR-483 directly targets NDRG2 to promote biological progression of colorectal cancer cells (10). miR-204-5p is an upstream factor of NDRG3. miR-204-5p inhibits cell proliferation and invasion in liver cancer and acute myeloid leukemia (44,45). miR-204-5p can promote drug resistance in gastric cancer and melanoma (46,47). The aforementioned studies show that miR-204-5p has different expression and roles in different types of cancer. Here, miR-204-5p inhibited cell proliferation and decreased drug resistance. IC_{50} following co-transfection with NDRG3 and miR-204-5p-mimic was 1.85 times higher than in cells transfected only with miR-204-5p-mimic. Therefore, NDRG3 can reverse the effects of miR-204-5p.

Grassi *et al* (48) demonstrated that the WNT/β-catenin involvement is a key factor in drug resistance. β-catenin primarily exerts its function in the nucleus as a downstream transcription factor of Wnt signaling (49). Wnt/β-catenin signaling is involved in NDRG3-mediated HCC metastasis (37). When cells receive Wnt signals, the degradation pathway is inhibited, leading to stabilization and nuclear accumulation of β-catenin protein. Nuclear β-catenin exerts further biological roles (50,51). NDRG3 is primarily localized in the cytoplasm and is a key factor required for drug resistance (52). The present study found that NDRG3 and β-catenin can interact in the cytoplasm. Wnt/β-catenin regulates the transcription of ABCB1 (β-catenin) in CML multidrug resistance (53). Addition of cholamine to KBM5-mesenchymal stromal cell (MSC) co-culture restores the effect of IM by abolishing MSC-mediated induction of β-catenin; inhibition of β-catenin signaling in CML cells by chidamide and IM inhibits proliferation of TKI-resistant cells and increases chemosensitivity (54). The present findings suggested that β-catenin was involved in drug resistance; accumulation of β-catenin increased in the nucleus after overexpression of NDRG3. Downstream factors of β-catenin promote cell proliferation and drug resistance. The effect of NDRG3 was alleviated after adding β-catenin inhibitor. In addition, the effects of NDRG3 on cell proliferation were reversed by β-catenin. IC_{50} after co-transfection with si-NDRG3 and β-catenin overexpression was 1.64 times greater than in cells transfected with si-NDRG3 alone. si-β-catenin affects NDRG3, thereby weakening IM resistance of NDRG3.

A limitation of the present study is that certain drug-resistant cells survive at high concentrations of IM, which may hinder the recovery of patients with CML patients. An additional limitation is that the formation of IM-resistant cells is critical for overcoming CML relapse; further studies should be performed at the single-cell level to obtain more detailed data and determine the underlying mechanism. Immunofluorescence images with higher magnification should be captured.

Future studies should investigate primary tumors in a mouse model of leukemia. The mechanism by which NDRG3 affects β-catenin needs further study. CML is a model disease with a long history (55). Identifying and understanding the biological characteristics of CML stem cells is a key research field (56). The role of NDRG3 in CML stem cells should be investigated in future. In addition, it was hypothesized that K562 cells serve a role in IM resistance; this should be investigated in the future.

In conclusion, the present study found that NDRG3 increased nuclear accumulation of β-catenin, thus increasing K/G cell proliferation and enhancing drug resistance. Moreover, miR-204-5p regulated NDRG3. The present study provides a basis for alleviating drug resistance in CML.

Acknowledgements

Not applicable.

Funding

The present study was supported by The Support Plan for Youth Entrepreneurship and Technology of Colleges and Universities in Shandong (grant no. 2019KJK014), The National Natural Science Foundation of China (grant nos. 81800169 and 82002604), The Shandong Science and Technology Committee (grant nos. ZR2019MH022, ZR2020QH221 and ZR2020KH015), The Shandong Province Taishan Scholar Project (grant no. ts201712067), The Foundation of Binzhou Medical University (grant no. BY2021LCX04) and The Shandong Province Yantai Science and Technology Project (grant no. 2022YD075).

Availability of data and materials

The datasets used and/or analyzed during the current study are available from the corresponding author on reasonable request.

Authors' contributions

SX, YL, YS, XW and BY designed the study, performed data analysis and revised the paper. XY and XL collected clinical samples. XW and SR performed cell culture experiments. HS, YY, GS, YL and PW analyzed and interpreted data. XW and YL confirm the authenticity of all the raw data. All authors have read and approved the final manuscript.

Ethics approval and consent to participate

The present study protocol was approved by the Animal Ethics Committee of Binzhou Medical University and the Medical Ethics Committee of Binzhou Medical University (Yantai, China) (approval number: 2020-10-06). The written informed consent was obtained from all subjects.

Patient consent for publication

Not applicable.

Competing interests

The authors declare that they have no competing interests.

References

1. Gale RP: Radiation and leukaemia: Which leukaemias and what doses? Blood Rev 58: 101017, 2023.
2. Radich J, Yeung C and Wu D: New approaches to molecular monitoring in CML (and other diseases). Blood 134: 1578-1584, 2019.
3. Berman E: How I treat chronic-phase chronic myelogenous leukemia. Blood 139: 3138-3147, 2022.
4. Navabi A, Akbari B, Abdalsamadi M and Naseri S: The role of microRNAs in the development, progression and drug resistance of chronic myeloid leukemia and their potential clinical significance. Life Sci 296: 120437, 2022.
5. Hershkovitz-Rokah O, Modai S, Pasmanik-Chor M, Toren A, Shomron N, Raanani P, Shpilberg O and Granot G: Restoration of miR-424 suppresses BCR-ABL activity and sensitizes CML cells to imatinib treatment. Cancer Lett 360: 245-256, 2015.
6. Zeng F, Peng Y, Qin Y, Wang J, Jiang G, Feng W and Yuan Y: Wee1 promotes cell proliferation and imatinib resistance in chronic myeloid leukemia via regulating DNA damage repair dependent on ATM-γH2AX-MDC1. Cell Commun Signal 20: 199, 2022.
7. Lee GY, Shin SH, Shin HW, Chun YS and Park JW: NDRG3 lowers the metastatic potential in prostate cancer as a feedback controller of hypoxia-inducible factors. Exp Mol Med 50: 1-13, 2018.
8. Schonkeren SL, Massen M, van der Horst R, Koch A, Vaes N and Melotte V: Nervous NDRGs: The N-myc downstream-regulated gene family in the central and peripheral nervous system. Neurogenetics 20: 173-186, 2019.
9. Sohn HA, Lee DC, Park A, Kang M, Yoon BH, Lee CH, Kim YH, Oh KJ, Kim CY, Park SH, *et al*: Glycogen storage disease phenotypes accompanying the perturbation of the methionine cycle in NDRG3-deficient mouse livers. Cells 11: 1536, 2022.
10. Sun X, Li K, Wang H, Xia Y, Meng P and Leng X: MiR-483 promotes colorectal cancer cell biological progression by directly targeting NDRG2 through regulation of the PI3K/AKT signaling pathway and epithelial-to-mesenchymal transition. J Healthc Eng 2022: 4574027, 2022.
11. Li T, Sun R, Lu M, Chang J, Meng X and Wu H: NDRG3 facilitates colorectal cancer metastasis through activating Src phosphorylation. Onco Targets Ther 11: 2843-2852, 2018.
12. Park KC, Lee DC and Yeom YI: NDRG3-mediated lactate signaling in hypoxia. BMB Rep 48: 301-302, 2015.
13. Yu C, Hao X, Zhang S, Hu W, Li J, Sun J and Zheng M: Characterization of the prognostic values of the NDRG family in gastric cancer. Therap Adv Gastroenterol 12: 1756284819858507, 2019.
14. Kim KR, Kim KA, Park JS, Jang JY, Choi Y, Lee HH, Lee DC, Park KC, Yeom YI, Kim HJ and Han BW: Structural and biophysical analyses of human N-Myc Downstream-Regulated Gene 3 (NDRG3) protein. Biomolecules 10: 90, 2020.
15. Lee DC, Sohn HA, Park ZY, Oh S, Kang YK, Lee KM, Kang M, Jang YJ, Yang SJ, Hong YK, *et al*: A lactate-induced response to hypoxia. Cell 161: 595-609, 2015.
16. Zhang J and Zhang Q: VHL and hypoxia signaling: Beyond HIF in cancer. Biomedicines 6: 35, 2018.
17. Si W, Shen J, Du C, Chen D, Gu X, Li C, Yao M, Pan J, Cheng J, Jiang D, *et al*: A miR-20a/MAPK1/c-Myc regulatory feedback loop regulates breast carcinogenesis and chemoresistance. Cell Death Differ 25: 406-420, 2018.
18. Hill M and Tran N: miRNA interplay: Mechanisms and consequences in cancer. Dis Model Mech 14: dmm047662, 2021.
19. Xu C, Fu H, Gao L, Wang L, Wang W, Li J, Li Y, Dou L, Gao X, Luo X, *et al*: BCR-ABL/GATA1/miR-138 mini circuitry contributes to the leukemogenesis of chronic myeloid leukemia. Oncogene 33: 44-54, 2014.
20. Feng X, Zou B, Nan T, Zheng X, Zheng L, Lan J, Chen W and Yu J: MiR-25 enhances autophagy and promotes sorafenib resistance of hepatocellular carcinoma via targeting FBXW7. Int J Med Sci 19: 257-266, 2022.
21. Yao S, Yin Y, Jin G, Li D, Li M, Hu Y, Feng Y, Liu Y, Bian Z, Wang X, *et al*: Exosome-mediated delivery of miR-204-5p inhibits tumor growth and chemoresistance. Cancer Med 9: 5989-5998, 2020.
22. Yu J, Shen J, Qiao X, Cao L, Yang Z, Ye H, Xi C, Zhou Q, Wang P and Gong Z: SNHG20/miR-140-5p/NDRG3 axis contributes to 5-fluorouracil resistance in gastric cancer. Oncol Lett 18: 1337-1343, 2019.
23. Du Z, Niu S, Xu X and Xu Q: MicroRNA31-NDRG3 regulation axes are essential for hepatocellular carcinoma survival and drug resistance. Cancer Biomark 19: 221-230, 2017.
24. Paller AS: Wnt signaling in focal dermal hypoplasia. Nat Genet 39: 820-821, 2007.
25. Wang Z, Li Z and Ji H: Direct targeting of β-catenin in the Wnt signaling pathway: Current progress and perspectives. Med Res Rev 41: 2109-2129, 2021.
26. Liu Y, Zhuang H, Cao F, Li J, Guo Y, Zhang J, Zhao Q and Liu Y: Shc3 promotes hepatocellular carcinoma stemness and drug resistance by interacting with β-catenin to inhibit its ubiquitin degradation pathway. Cell Death Dis 12: 278, 2021.
27. Valenta T, Hausmann G and Basler K: The many faces and functions of β-catenin. EMBO J 31: 2714-2736, 2012.
28. Schunk SJ, Floege J, Fliser D and Speer T: WNT-β-catenin signalling-a versatile player in kidney injury and repair. Nat Rev Nephrol 17: 172-184, 2021.
29. Yu F, Yu C, Li F, Zuo Y, Wang Y, Yao L, Wu C, Wang C and Ye L: Wnt/β-catenin signaling in cancers and targeted therapies. Signal Transduct Target Ther 6: 307, 2021.
30. Cui C, Zhou X, Zhang W, Qu Y and Ke X: Is β-catenin a druggable target for cancer therapy? Trends Biochem Sci 43: 623-634, 2018.
31. Liu J, Xiao Q, Xiao J, Niu C, Li Y, Zhang X, Zhou Z, Shu G and Yin G: Wnt/β-catenin signalling: Function, biological mechanisms, and therapeutic opportunities. Signal Transduct Target Ther 7: 3, 2022.
32. Gao Y, Han T, Han C, Sun H, Yang X, Zhang D and Ni X: Propofol regulates the TLR4/NF-κB pathway through miRNA-155 to protect colorectal cancer intestinal barrier. Inflammation 44: 2078-2090, 2021.
33. McLoughlin R, Berthon BS, Rogers GB, Baines KJ, Leong LE, Gibson PG, Williams EJ and Wood LG: Soluble fibre supplementation with and without a probiotic in adults with asthma: A 7-day randomised, double blind, three way cross-over trial. EBioMedicine 46: 473-485, 2019.
34. Perugorria MJ, Olaizola P, Labiano I, Esparza-Baquer A, Marzioni M, Marin JJ, Bujanda L and Banales JM: Wnt-β-catenin signalling in liver development, health and disease. Nat Rev Gastroenterol Hepatol 16: 121-136, 2019.
35. Ma W, Zhao X, Xue N, Gao Y and Xu Q: The LINC01410/miR-122-5p/NDRG3 axis is involved in the proliferation and migration of osteosarcoma cells. IUBMB Life 73: 705-717, 2021.

36. Ma J, Liu S, Zhang W, Zhang F, Wang S, Wu L, Yan R, Wu L, Wang C, Zha Z and Sun J: High expression of NDRG3 associates with positive lymph node metastasis and unfavourable overall survival in laryngeal squamous cell carcinoma. Pathology 48: 691-696, 2016.
37. Shi J, Zheng H and Yuan L: High NDRG3 expression facilitates HCC metastasis by promoting nuclear translocation of β-catenin. BMB Rep 52: 451-456, 2019.
38. Rosa Fernandes L, Stern AC, Cavaglieri RC, Nogueira FC, Domont G, Palmisano G and Bydlowski SP: 7-Ketocholesterol overcomes drug resistance in chronic myeloid leukemia cell lines beyond MDR1 mechanism. J Proteomics 151: 12-23, 2017.
39. Ma W, Zhu M, Wang B, Gong Z, Du X, Yang T, Shi X, Dai B, Zhan Y, Zhang D, *et al*: Vandetanib drives growth arrest and promotes sensitivity to imatinib in chronic myeloid leukemia by targeting ephrin type-B receptor 4. Mol Oncol 16: 2747-2765, 2022.
40. Nagata K, Kawakami T, Kurata Y, Kimura Y, Suzuki Y, Nagata T, Sakuma Y, Miyagi Y and Hirano H: Augmentation of multiple protein kinase activities associated with secondary imatinib resistance in gastrointestinal stromal tumors as revealed by quantitative phosphoproteome analysis. J Proteomics 115: 132-142, 2015.
41. Saha M and Sarkar A: Review on multiple facets of drug resistance: A rising challenge in the 21st century. J Xenobiot 11: 197-214, 2021.
42. Sun X, Niu X, Chen R, He W, Chen D, Kang R and Tang D: Metallothionein-1G facilitates sorafenib resistance through inhibition of ferroptosis. Hepatology 64: 488-500, 2016.
43. Wang XY, Sun GB, Wang YJ and Yan F: Emodin inhibits resistance to Imatinib by downregulation of Bcr-Abl and STAT5 and allosteric inhibition in chronic myeloid leukemia cells. Biol Pharm Bull 43: 1526-1533, 2020.
44. Xue F and Che H: The long non-coding RNA LOC285758 promotes invasion of acute myeloid leukemia cells by down-regulating miR-204-5p. FEBS Open Bio 10: 734-743, 2020.
45. Jiang G, Wen L, Zheng H, Jian Z and Deng W: miR-204-5p targeting SIRT1 regulates hepatocellular carcinoma progression. Cell Biochem Funct 34: 505-510, 2016.
46. Xiao YF, Li BS, Liu JJ, Wang SM, Liu J, Yang H, Hu YY, Gong CL, Li JL and Yang SM: Role of lncSLCO1C1 in gastric cancer progression and resistance to oxaliplatin therapy. Clin Transl Med 12: e691, 2022.
47. Díaz-Martínez M, Benito-Jardón L, Alonso L, Koetz-Ploch L, Hernando E and Teixidó J: miR-204-5p and miR-211-5p contribute to BRAF inhibitor resistance in melanoma. Cancer Res 78: 1017-1030, 2018.
48. Grassi S, Palumbo S, Mariotti V, Liberati D, Guerrini F, Ciabatti E, Salehzadeh S, Baratè C, Balducci S, Ricci F, *et al*: The WNT pathway is relevant for the BCR-ABL1-independent resistance in chronic myeloid leukemia. Front Oncol 9: 532, 2019.
49. Ding L, Chen Q, Chen K, Jiang Y, Li G, Chen Q, Bai D, Gao D, Deng M, Zhang H and Xu B: Simvastatin potentiates the cell-killing activity of imatinib in imatinib-resistant chronic myeloid leukemia cells mainly through PI3K/AKT pathway attenuation and Myc downregulation. Eur J Pharmacol 913: 174633, 2021.
50. Liu F, Kohlmeier S and Wang CY: Wnt signaling and skeletal development. Cell Signal 20: 999-1009, 2008.
51. Sinha A, Fan VB, Ramakrishnan AB, Engelhardt N, Kennell J and Cadigan KM: Repression of Wnt/β-catenin signaling by SOX9 and mastermind-like transcriptional coactivator 2. Sci Adv 7: eabe0849, 2021.
52. Nakamura K, Kustatscher G, Alabert C, Hödl M, Forne I, Völker-Albert M, Satpathy S, Beyer TE, Mailand N, Choudhary C, *et al*: Proteome dynamics at broken replication forks reveal a distinct ATM-directed repair response suppressing DNA double-strand break ubiquitination. Mol Cell 81: 1084-1099.e6, 2021.
53. Huang Y, Yuan C, Liu Q and Wang L: KIF23 promotes autophagy-induced imatinib resistance in chronic myeloid leukaemia through activating Wnt/β-catenin pathway. Clin Exp Pharmacol Physiol 49: 1334-1341, 2022.
54. He B, Wang Q, Liu X, Lu Z, Han J, Pan C, Carter BZ, Liu Q, Xu N and Zhou H: A novel HDAC inhibitor chidamide combined with imatinib synergistically targets tyrosine kinase inhibitor resistant chronic myeloid leukemia cells. Biomed Pharmacother 129: 110390, 2020.
55. Minciacchi VR, Kumar R and Krause DS: Chronic myeloid leukemia: A model disease of the past, present and future. Cells 10: 117, 2021.
56. Houshmand M, Simonetti G, Circosta P, Gaidano V, Cignetti A, Martinelli G, Saglio G and Gale RP: Chronic myeloid leukemia stem cells. Leukemia 33: 1543-1556, 2019.

Copyright © 2023 Wang et al. This work is licensed under a Creative Commons Attribution-NonCommercial-NoDerivatives 4.0 International (CC BY-NC-ND 4.0) License.